

# Optical fiber strain sensor with extended dynamic range based on specklegrams

Luis Rodriguez-Cobo<sup>1</sup>, Mauro Lomer, Adolfo Cobo, Jose-Miguel  
Lopez-Higuera

*Photonics Engineering Group. University of Cantabria. 39005, Santander, Spain*

---

## Abstract

In this paper, a processing scheme based on the morphological similarities of speckle patterns is proposed to extend the dynamic range of Fiber Specklegram Sensors (FSS). The method has been applied to a low cost FSS demonstrating its good performance to extend the dynamic range of strain measurements. The scheme analyzes the pattern energy distribution to establish the current modal state of the FSS and employs the correlation value with the reference modal state specklegram to determine the fine strain measurements. The achieved results exhibit a very high performance, making this low cost technology applicable to structural monitoring.

*Keywords:* Polymer optical fiber, Specklegram, Sensor, Low cost, Extended range

---

## 1. Introduction

Optical fiber sensors have been widely employed for structural health monitoring purposes. Particularly, those based on silica have been employed in such different ways such as distributed sensing (Brillouin, Raman...) or punctual sensors (Fiber Bragg Gratings, Microbendings ...). They have

---

\*Corresponding author: Tel.: +34 942 200877; fax.: +34 942 200877.

*Email addresses:* [luis.rodriiguez@unican.es](mailto:luis.rodriiguez@unican.es) (Luis Rodriguez-Cobo),  
[lomerm@unican.es](mailto:lomerm@unican.es) (Mauro Lomer), [adolfo.cobo@unican.es](mailto:adolfo.cobo@unican.es) (Adolfo Cobo),  
[miguel.lopezhiguera@unican.es](mailto:miguel.lopezhiguera@unican.es) (Jose-Miguel Lopez-Higuera)

<sup>1</sup>Current address: Photonics Engineering Group. University of Cantabria. Av Los Castros S/N, 39005, Santander, Spain

many advantages, but their applicability can be sometimes limited by different factors such as cost, sensitivity or repeatability. On the other hand, different sensor systems based on Polymer optical fibers (POF) have been proposed, exhibiting the benefits of this technology for sensing purposes. Although optical loss in POFs is much higher than in conventional glass fibers, robustness, ease of handling and low cost have made them an attractive option for sensing applications such as health monitoring in civil engineering or structures with large shape changes [1, 2]. In this regard, POFs exhibit advantages including high elastic strain limits, high fracture toughness, and excellent flexibility and adaptability. Furthermore, there is a wide variety of multimode fiber core diameters available. More specifically, sensors using these fibers have been successfully demonstrated such as Fiber Specklegram Sensors (FSS) [3–7] that highlight, with a remarkable sensitivity to external perturbations and, due to cost reduction in the electronics, with possibility of being implemented as a low cost technology but maintaining an extremely high sensitivity.

Using FSS, several parameters have been successfully measured such as vibration [3, 7], micrometric displacements [4, 5], temperature [5] or angular alignments [6]. Most of the reported applications are far from measuring suitable parameters for structural monitoring applications due to the limited dynamic range or the oversensitivity and cross-sensitivity of the FSS principle. Nevertheless, a strain measurement scheme based on FSS has been reported [8] by adhering multimode optical fibers to a cantilever beam and measuring the speckle intensity variation, that is proportional to the applied strain. The achieved results exhibit a good linearity, but this scheme is limited in dynamic range because it is based in a weak perturbation approximation. In other works, some photorefractive materials are employed to stabilize the processed specklegrams [9, 10]. This effect can be applied to reduce the extra noise due to the typical oversensitivity of specklegrams and to extend the dynamic range for slow varying perturbations. Despite of the adaptation capabilities of the proposed schemes, the setup is not suitable for low cost applications.

In this work, a new processing scheme to extend the dynamic range of Fiber Specklegram Sensors is proposed and demonstrated. The proposed algorithm employs the morphological differences between two specklegrams under very different perturbations to determine key-specklegrams as reference points. The speckle intensity variation is computed to the closest key-specklegram and the absolute strain can be obtained by employing this par-

tial variation. A FSS has been embedded into a composite beam and several strain tests have been performed. The obtained specklegram sequence has been morphologically processed obtaining a very good performance. The proposed scheme is also suitable for applications where cost is a critical point.

## 2. Sensing principle

The speckle phenomenon in optical fibers has been treated by several authors [11–13]. It is generally considered that the number of speckles projected by a multimode optical fiber on a screen is approximately equal to the number of modes ( $M$ ) that supports the fiber [14]. For a step-index fiber, the number of modes is approximately  $M = V^2/2$  and for a graded-index fiber is  $M = V^2/4$ , where  $V$  is the normalized propagation constant. This value is defined as  $V = 2\pi a NA/\lambda$ , where  $NA$  is the numerical aperture of the fiber,  $\lambda$  the wavelength of the light source and  $a$  is the radius of the fiber core. For a multimode step-index fiber, the expression for  $M$  can be calculated by resolving the Helmholtz equation considering a plane wave rectilinearly polarized. Based on the ray model approximation, it can be considered that each mode has a different phase velocity caused by different optical paths and, at the output end of the fiber, each mode has a different spatial position.

When a coherent light is propagated through the fiber, the speckle phenomenon is defined as an interference between different modes and self-mode interaction [3]. The output speckle pattern (i.e. projected onto a screen) is composed of a large number of bright spots (approximately the number of modes  $M$ ) whose intensity varies slowly, mainly caused by environmental effects, but the total intensity of the speckle pattern remains constant.

Several changes in the fiber geometry and in the refraction index are caused when an external perturbation is applied to the fiber (such as temperature, pressure or strain). These changes also cause variations in the output speckle pattern distribution, but its total intensity remains constant. There is a model [3] that determines the relation between the speckle pattern variation and the perturbation to be measured. The model considers that the mode propagation and the mode interference are both modified by the perturbation ( $F(t)$ ), that is reflected in the speckle intensity variation. This model is limited to small perturbations and the intensity of each speckle  $I_i$  can be calculated as the integration of the spatial intensity function for each speckle area:

$$I_i = A_i \cdot \{1 + B_i \cdot [\cos(\delta_i) - F(t) \cdot \phi_i \cdot \sin(\delta_i)]\} \quad (1)$$

where  $A_i$  represents the self-mode interaction; and  $F(t)$ ,  $B_i$  and  $\delta_i$  define the interaction between different modes. Particularly,  $F(t)$  is the external perturbation of the fiber. The argument of the harmonic functions ( $\delta_i$ ) describes the difference in the propagation constant and the random phase of all the pairs of modes considered within the same speckle intensity  $I_i$ .  $A_i$ ,  $B_i$ ,  $\phi_i$  and  $\delta_i$  are constant values for any given  $i$ .

In order to extract the perturbation information ( $F(t)$ ), a differential processing method is applied to Eq. 1. The sum of the absolute value of the changes in all the signals is computed and can be described by:

$$\Delta I_T = \sum_{i=1}^N \left[ -A_i \cdot B_i \cdot \phi_i \cdot \frac{dF(t)}{dt} \cdot \sin(\delta_i) \right] = \left[ \sum_{i=1}^N C_i \cdot \sin(\delta_i) \right] \cdot \frac{dF(t)}{dt} \quad (2)$$

In Eq. 2 the term within the brackets sums all the components of the speckle pattern, so the sum will remain constant despite local variations (the total energy is maintained). Eq. 2 can be written as:

$$\Delta I_T = \frac{dI_T}{dt} = C \cdot \frac{dF(t)}{dt} = C \cdot \Delta F \quad (3)$$

Based on this approach, several sensors have been demonstrated [3, 8]. However, when the perturbation applied to the fiber is larger (not weak), the approach required to achieve Eq. 3 is not valid, so the method is very limited in dynamic range. In the described model, only the self-mode interaction and the mode-mode interaction are taken into account, while the physical process is much more complex. The influence of the radiated modes, propagation losses, bendings or micro-bendings has been ignored so it can be assumed that more complex phenomena besides the self-mode and mode-mode interaction are produced. These effects in propagating waveguides have been analyzed by using the perturbation theory [15]. By observing a speckle pattern evolution, when a large perturbation is applied, the individual speckle area and position change indicating that the modal state energy is being re-distributed. Obtaining an analytical description of all these phenomena is not a trivial task. However, a correlation between the speckle distribution and the external perturbation can be computed using the available computer methods.

### 3. Morphological processing

As detailed in the previous section and demonstrated in [8], the specklegram correlation is proportional to the strain but just when  $\Delta F$  is small enough. The correlation between specklegrams is useful within the same modal state where it is proportional to the external perturbation. Given that the correlation is not an useful metric to compare two specklegrams of different modal states, other approach is required. The morphological processing obtains the distribution of the different bright speckles and employs it to “define” the specklegram characteristics. Thus, to extend the dynamic range through different modal states, the correlation term may be computed to different Key-Specklegrams (KSs) associated with the different modal states. These KSs are determined during the sensor calibration ramp and they are associated with a strain value, establishing different local reference points corresponding to the different modal states. The wrong determination of the KSs may lead to a wrong sensor performance.

In the morphological processing the specklegram is converted to a binary image (using a threshold) and the different white spots (correspondent to bright speckles) are defined from their X-Y position and area. After the thresholding, a circular averaging filter is employed to reduce the sharpness of the obtained dots. This filtering creates a clustering effect by combining several small dots into a bigger one reducing the final noise. The noise reduction is more significant when the bright speckles are close to the threshold, where a big spot can be decomposed into several smaller ones.

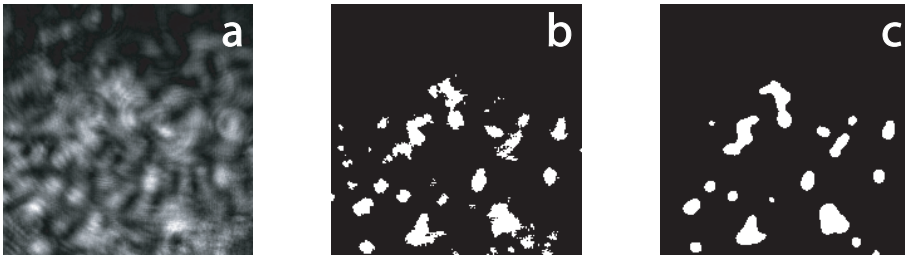


Figure 1: Preprocessing steps. A 200x200 pixels gray level image of a specklegram (a). The same specklegram thresholded (b) and filtered (c).

The obtained spots are sorted by area, making the larger ones more relevant. The list of sorted spots is the geometrical representation of a specklegram and it defines its high level morphological structure. Once the structure

of a specklegram has been determined, the spots with the larger area of both specklegrams are compared to the closest ones taking into account their position. After having established the spot correspondence, their area difference is calculated and normalized against the total area. This value is related to the amount of coincident bright speckles between the two specklegrams, which is related to the coincidence (or not) of the modal state. A high error value indicates a completely different bright speckle distribution, what implies a different modal state.

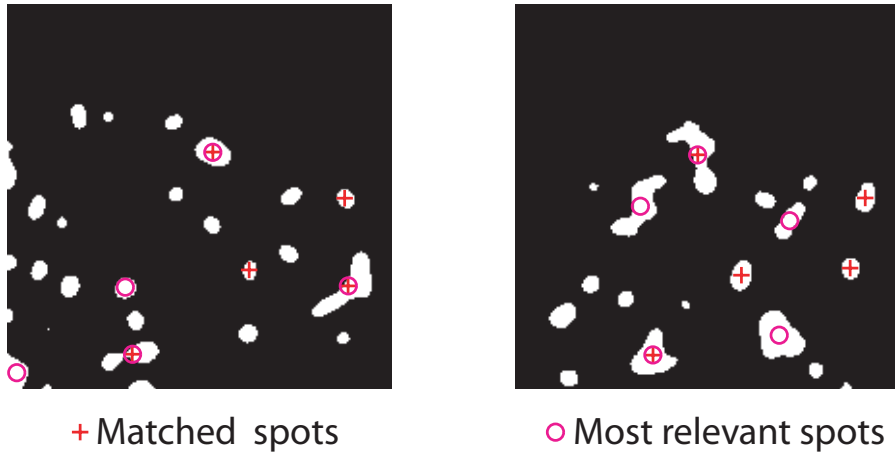


Figure 2: Morphological comparison between two specklegrams of different modal states.

In Fig.2 two specklegrams of different modal states are depicted. The five spots with the larger area (most relevant) are marked with circles for both images. The five most relevant coincident spots between specklegrams are also marked with crosses. In this case, most of the bright speckle area is not coincident (three of the most relevant spots of the right specklegram are not matched) so the obtained value is high, indicating a different modal state.

Strain specklegram sensors need to be calibrated before their application thus, a calibration procedure is required. During this step, a controlled strain ramp is applied to the POF while the specklegrams are acquired. When the applied perturbation (i.e. strain) is high enough, the modal state is not maintained and the speckle intensity variation ( $\Delta I_T$ ) does not replicates the perturbation. The morphological metric is employed to identify the different modal states during the calibration ramp and to establish their correspondent

KSs to have local reference points (KSs) where the speckle intensity variation will be calculated. This parameter, for two specklegrams of  $N \times M$  pixels, can be defined as follows:

$$\Delta I_T\{i, j\} = \frac{1}{K \cdot N \cdot M} \sum_{n=1}^N \sum_{m=1}^M |p_{n,m}^i - p_{n,m}^j| \quad (4)$$

where  $K$  is the full scale value of the specklegram colormap (i.e  $K = 255$  for 8-bit grayscale) and  $p_{n,m}$  corresponds to the pixel of the  $n, m$  position of the specklegram  $i$  or  $j$ . Applying this notation to Eq. 3, the perturbation value of the  $i$ -th specklegram under a weak perturbation having the initial specklegram as reference can be obtained with:

$$\Delta F\{i\} = \frac{1}{C} \cdot \Delta I_T\{0, i\} = L_0 \cdot \Delta I_T\{0, i\} \quad (5)$$

being  $L_0$  the proportionality constant (slope) between the speckle intensity variation (between the  $i$ -th and the first specklegram). During the sensor calibration step, different KSs are detected and their associated slopes ( $L_{KS(k)}$ ) and strain values ( $S_{KS(k)}$ ) are also saved. Consequently, when a new specklegram is available,  $I(i)$ , can be evaluated in terms of its closest KS under the weak perturbation assumption. The speckle intensity variation of the incoming specklegram is calculated with all the stored KSs. The closest is employed as a strain reference and, with its slope, the strain value can be calculated. The second closer KS is employed to indicate the direction ( $d(i)$ ) of the calculated strain offset. The absolute strain value can be obtained as:

$$Strain(i) = \Delta F\{i\} = S_{KS(i)} + d(i) \cdot L_{KS(i)} \cdot I_T\{KS(i), i\} \quad (6)$$

where  $KS(i)$  denotes the KS associated with the  $I(i)$  specklegram;  $S_{KS(i)}$  and  $L_{KS(i)}$  denote the strain value and slope correspondent to the KS associated with the  $i$ -th specklegram and  $d(i) \in [-1, 1]$  describes the intensity variation direction (positive or negative). However, for the incoming specklegrams that falls in the middle of two KSs, the final strain value is taken as the mean value of both references. This effect is detected when the two closest KSs intensity variations are very similar. The absolute strain value under this assumption is computed as:

$$Strain(i) = \frac{1}{2} \cdot \left[ S_{KS(i)_1} + d(i) \cdot L_{KS(i)_1} \cdot I_T\{KS(i)_1, i\} \right] + \frac{1}{2} \cdot \left[ S_{KS(i)_2} - d(i) \cdot L_{KS(i)_2} \cdot I_T\{KS(i)_2, i\} \right] \quad (7)$$

where  $KS(i)_1$  and  $KS(i)_2$  denote the two KS with a lower intensity variation with the  $i$ -th specklegram. This averaging step reduces the amount of noise in transition areas where the distance (intensity variation) between two specklegrams is very close.

#### 4. Experiments and results

The described processing scheme has been tested with an experimental strain measurement. For this purpose a Glass Fiber Reinforced Plastic (GFRP) beam has been manufactured with an embedded easy-to-handle POF. Despite several POFs with a diameter of few micrometers are commercially available, for FSSs, larger core diameters are required. Particularly, wide set of commercial POFs for FSS can be found with diameters from  $50 \mu m$  to  $3 mm$ . The chosen POF has a core diameter of  $d_c = 50 \mu m$  and an external diameter of  $d_o = 250 \mu m$ . A graded-index profile has been also chosen to reduce the number of modes, thus decreasing the noise. A Fiber Bragg Grating written in a standard telecommunications fiber has been also embedded to obtain the strain reference for the calibration ramp and further measurements. The beam has a constant thickness of 2 mm and a final size of 400x60 mm.

##### 4.1. Experimental setup

The beam is fixed in one side and the other is attached to a mobile part connected to a screw that stretches the whole beam uniformly. One edge of the POF is connected to a cheap laser diode and the other side is connected to a CCD camera (Pixelink PL-A741). The FBG is attached to a Fibersensing FS4200 interrogation unit to obtain the reference strain value of each experiment. The whole setup is depicted in Fig. 3.

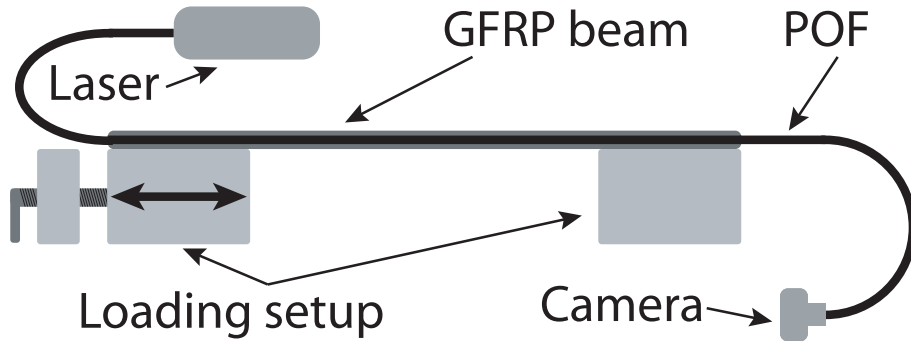


Figure 3: Experimental setup. The POF is attached to a laser diode and a CCD camera. The FBG is interrogated using a commercial unit.

Several increasing and decreasing strain ramps were applied to the beam provoking a maximum deformation of  $\Delta s \approx 200\mu\epsilon$ . The strain was uniformly distributed along the 400 mm of the stretched beam. During the experiment, the first increasing ramp has been employed for the sensor calibration. The rest of the measured values have been used to study the performance of the sensor out of the calibration ramp. Specklegrams were captured at 25 frames per second.

#### 4.2. Results and discussion

The morphological processing scheme is applied to obtain the KSs of an increasing strain ramp. For the analyzed data, the processing scheme has obtained five KSs during the calibration step (the last one is added to determine the direction of the strain values above the last KS). Once the calibration procedure was finished, the same specklegrams sequence was employed to estimate the strain using the proposed method.

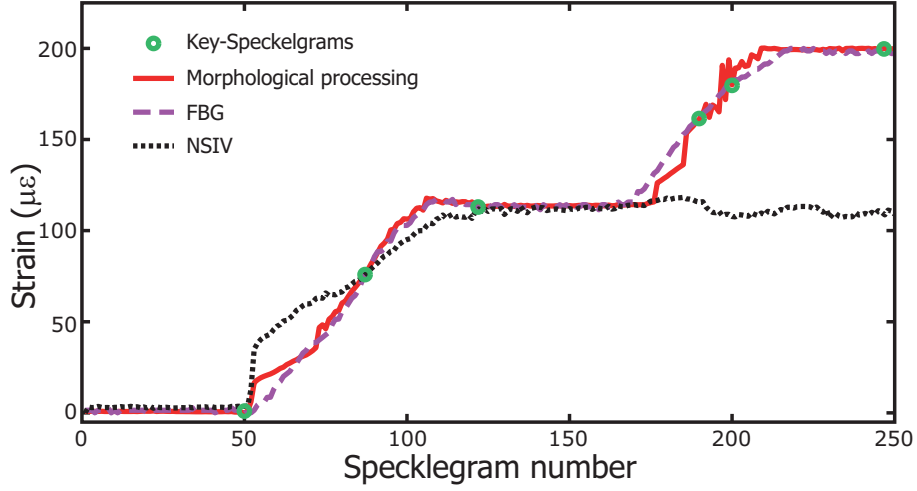


Figure 4: Calibration strain ramp. Strain values obtained with the morphological processing (solid line) are compared against the strain measured with the FBG (dashed line). The values proportional to the speckle intensity variation are also plotted (dotted line).

In Fig.4 the five identified KSs (circles) are plotted over the reference strain value (obtained with the FBG). The strain values obtained using the morphological processing are also depicted (solid line) and compared to the correlation processed ones (dotted line). The correlation method (Normalized Speckle Intensity Variation, NSIV) is described in [8] and it is limited to small deformations because it is only valid for the same modal state. As can be observed in Fig. 4, when the deformation is enough to change the modal state, the correlation method is useless because specklegrams cannot be directly compared. The achieved accuracy within the calibration ramp of the morphological scheme is remarkable, being always under  $max(\Delta s) \approx 29.0\mu\epsilon$  with a mean error of  $\overline{\Delta s} \approx 5.6\mu\epsilon$ , good enough for the majority of structural applications. However, the presented case is an optimistic situation when the application scenario is exactly the same as the testing one, thus, the same calibration parameters have been also employed to test the sensor with other strain ramps.

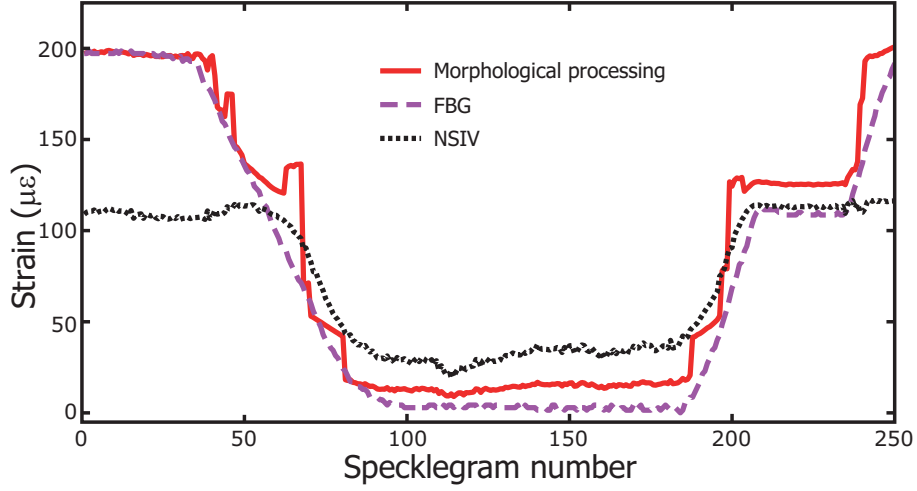


Figure 5: Strain values obtained with the morphological method (solid line) are compared against the strain measured with the FBG (dashed line) during strain ramps not included in the calibration. The values proportional to the speckle intensity variation are also plotted (dotted line).

A more realistic scenario is depicted in Fig.5 where the calibration parameters obtained in the previous ramp (Fig.4) have been applied to process specklegrams from other increasing and decreasing ramps. The KSs employed during this test are the same ones established during the calibration test. Morphological processed values (solid line) are plotted against the strain reference (dashed line) and the NSIV values (dotted line). The accuracy of the morphological method is not as good as the previous one, but it still is remarkably good for many structural applications, having a mean strain error of  $\overline{\Delta s} \approx 13.2\mu\epsilon$  and a maximum of  $\max(\Delta s) \approx 65.1\mu\epsilon$ . The worst cases are located during a transition between two reference KSs. This particular test indicates the suitability of the proposed processing scheme to work with a good response out of the calibration area, despite the noisy nature of the specklegram sensors. Besides, the maximum strain error is obtained during the transition between KSs when distances to both references are larger but it is not proportional to the sensor dynamic range.

Several factors are contributing to the final error, but one of the most significant is to light up the sensor with a multimode POF which varies the modal state before reaching the sensing area. This problem can be reduced by using a monomode fiber to carry the light to the sensing area, as proposed

in [8], or by locating the CCD camera right at the end of the sensing area, reducing extra perturbations. Similar results can be obtained using also low-cost techniques such as intensity based POF sensors [2], however Fiber Specklegram Sensors (FSS) can simplify the sensing head, what makes their installation easier.

Despite the obtained accuracy, using the correlation term to calculate the strain deviation in the morphological processing, is good enough for many applications, it can be improved by employing other comparison methods less noise dependent. The morphological scheme has been also tried as a method to obtain the strain deviation over a KS but, due to its noise immunity, it renders useless to perform this task. Some trade-off between noise immunity (morphological scheme) and sensitiveness (correlation) is required for a metric to obtain strain from specklegrams in real scenarios.

The dynamic range of the proposed technique is mainly limited on the KSs detection, when two equal KSs arise from the calibration ramp. Having identical KSs may lead the strain reconstruction to a wrong value. The probability of reaching two equal KSs is given by several factors such as the number of speckles of the specklegrams (proportional to the number of modes of an optical fiber) or the captured spot area and resolution. Based on the experimental tests, the probability of reaching two equal KSs with the proposed setup is very low, enabling this technique to be applied to full-range applications (i.e. 5000  $\mu\epsilon$ ) without modifying the setup

## 5. Conclusions

In this work, a morphological processing method to enhance the dynamic range of Specklegram strain sensors is proposed and demonstrated. The proposed method analyzes the geometrical properties of the specklegram to determine if the modal state of the hosting multimode fiber remains the same. Once the working range of each modal state is established (given by its associated Key-Specklegram), the correlation between the incoming specklegram and the KS is employed to obtain the absolute strain value. The processing scheme has been experimentally checked, exhibiting a great accuracy even with specklegrams not considered in the calibration steps, obtaining a final mean error of  $\overline{\Delta s} \approx 13.2\mu\epsilon$ . A low cost implementation of the proposed scheme is possible, enabling this method for different sensing purposes.

## Acknowledgments

Special thanks to Dr. Mirapeix Serrano for his support and reviews and to Roberto Perez Sierra for his valuable collaboration with the experimental works. This work has been supported by the project TEC2010-20224-C02-02 and grant AP2009-1403.

## References

- [1] K. Peters, Polymer optical fiber sensors: A review, *Smart materials and structures* 20 (1) (2010) 013002.
- [2] K. Kuang, S. Quek, C. Koh, W. Cantwell, P. Scully, Plastic optical fibre sensors for structural health monitoring: a review of recent progress, *Journal of sensors* 2009.
- [3] W. Spillman Jr, B. Kline, L. Maurice, P. Fuhr, Statistical-mode sensor for fiber optic vibration sensing uses, *Applied optics* 28 (15) (1989) 3166–3176.
- [4] F. Yu, M. Wen, S. Yin, C. Uang, Submicrometer displacement sensing using inner-product multimode fiber speckle fields, *Applied optics* 32 (25) (1993) 4685–4689.
- [5] K. Pan, C. Uang, F. Cheng, F. Yu, Multimode fiber sensing by using mean-absolute speckle-intensity variation, *Applied optics* 33 (10) (1994) 2095–2098.
- [6] S. Yin, P. Purwosumarto, F. Yu, Application of fiber specklegram sensor to fine angular alignment, *Optics communications* 170 (1) (1999) 15–21.
- [7] J. Leng, A. Asundi, Nde of smart structures using multimode fiber optic vibration sensor, *NDT and E International* 35 (1) (2002) 45–51.
- [8] Z. Zhang, F. Ansari, Fiber-optic laser speckle-intensity crack sensor for embedment in concrete, *Sensors and Actuators A: Physical* 126 (1) (2006) 107–111.
- [9] A. Kamshilin, T. Jaaskelainen, Y. Kulchin, Adaptive correlation filter for stabilization of interference-fiber-optic sensors, *Applied physics letters* 73 (6) (1998) 705–707.

- [10] J. Gomez, . Salazar, Self-correlation fiber specklegram sensor using volume characteristics of speckle patterns, *Optics and Lasers in Engineering*.
- [11] B. Crosignani, B. Daino, P. Porto, Speckle-pattern visibility of light transmitted through a multimode optical fiber, *JOSA* 66 (11) (1976) 1312–1313.
- [12] J. Goodman, E. Rawson, Statistics of modal noise in fibers: a case of constrained speckle, *Optics Letters* 6 (7) (1981) 324–326.
- [13] Y. Tremblay, B. Kawasaki, K. Hill, Modal noise in optical fibers: open and closed speckle pattern regimes, *Applied optics* 20 (9) (1981) 1652–1655.
- [14] G. Kaiser, *Optical Fiber Communications*, 2nd Edition, McGraw-Hill, NY, 1991, Ch. 2.
- [15] D. Marcuse, *Theory of dielectric optical waveguides*, New York, Academic Press, Inc., 1974. 267 p. 1.